

Maoquan Chu

# Laser-triggered Nanobiomaterials for Inhibiting Tumor Growth

 Springer

# Laser-triggered Nanobiomaterials for Inhibiting Tumor Growth

Maoquan Chu (储茂泉)

# Laser-triggered Nanobiomaterials for Inhibiting Tumor Growth

 Springer

Maoquan Chu (储茂泉)  
Research Center for Translational Medicine at Shanghai  
East Hospital, Frontier Science Center for Stem Cell Research  
and School of Life Sciences and Technology  
Tongji University  
Shanghai, China

ISBN 978-981-97-4219-6                      ISBN 978-981-97-4220-2 (eBook)  
<https://doi.org/10.1007/978-981-97-4220-2>

© The Editor(s) (if applicable) and The Author(s), under exclusive license to Springer Nature Singapore Pte Ltd. 2024

This work is subject to copyright. All rights are solely and exclusively licensed by the Publisher, whether the whole or part of the material is concerned, specifically the rights of translation, reprinting, reuse of illustrations, recitation, broadcasting, reproduction on microfilms or in any other physical way, and transmission or information storage and retrieval, electronic adaptation, computer software, or by similar or dissimilar methodology now known or hereafter developed.

The use of general descriptive names, registered names, trademarks, service marks, etc. in this publication does not imply, even in the absence of a specific statement, that such names are exempt from the relevant protective laws and regulations and therefore free for general use.

The publisher, the authors and the editors are safe to assume that the advice and information in this book are believed to be true and accurate at the date of publication. Neither the publisher nor the authors or the editors give a warranty, expressed or implied, with respect to the material contained herein or for any errors or omissions that may have been made. The publisher remains neutral with regard to jurisdictional claims in published maps and institutional affiliations.

This Springer imprint is published by the registered company Springer Nature Singapore Pte Ltd.  
The registered company address is: 152 Beach Road, #21-01/04 Gateway East, Singapore 189721, Singapore

If disposing of this product, please recycle the paper.

# Preface

Cancer cells can grow and form a cancerous tumor anywhere in the human body, so numerous (>100) types of tumors have been reported in the past to threaten human health seriously. How to overwhelm cancer cells is an issue of significant importance common all over the world. As any cancer therapy method is associated with its disadvantage, there is a need to introduce novel techniques for improving current cancer therapies with higher efficiency and reduced side effects.

Cancer cells and tumor tissue are more susceptible to heat than healthy cells and normal tissues. For example, cancer cells may get damaged if the temperature increases over 42–43 °C; whereas, normal cells may still survive even if the temperature reaches about 47 °C. Therefore, several thermal therapy techniques like whole-body, regional thermal therapy, and local hyperthermia have been introduced at a clinical level and are usually combined with other treatments such as chemotherapy to improve overall efficiency.

As an essential local thermal therapy method, red or near-infrared (NIR) laser-induced organic dyes- and nanomaterials-mediated photothermal therapy (PTT) have attracted significant attention. They are being investigated intensively for the last decade. In this technique, photothermal agents are injected intravenously or intratumorally into tumor-bearing animals or patients. The tumor is then exposed to a laser with a suitable wavelength and low power density. As long as the photothermal agents remain entrapped inside the tumor tissue, they can be irradiated with a laser repeatedly until tumor disappearance. This therapy exhibits few thermal injuries to normal tissues and shows no drug resistance. The photothermal effect only acts on tumor tissue to damage all types of cancer cells at elevated temperatures.

Selecting a suitable photothermal agent or developing a novel photothermal agent is vital for a successful PTT. Generally, low toxic materials with strong absorbance towards red or NIR light can be used as photothermal agents for PTT. Till now, many organic and inorganic materials which are from synthetic and natural sources have been investigated for their viability as photothermal agents. However, only a small fraction of photothermal agents such as magnetic iron oxide nanoparticles, gold nanostructures, and indocyanine green have been proven to possess great potential for clinic PTT, as other photothermal agents are mostly toxic to the

human body and/or are not biodegradable in vivo along with compromised photostability.

In this regard, magnetic iron oxide nanoparticles have been safely used in the human body for magnetic resonance imaging, drug targeted delivery, and alternating magnetic field (AMF)-triggered cancer thermal therapy. Therefore, magnetic iron oxide-mediated PTT can be moved easily towards clinical practice. Magnetic iron oxide possesses several unique characteristics that can be combined efficiently with PTT. These characteristics or functions include magnetic tumor-targeting under an external magnetic field, AMF-induced magneto-thermal conversion, dynamic magnetic field-induced mechanical moving (for generating mechanical force), rapid triggering of aggregation by a static magnetic field (for inducing the accumulation of death receptors or other receptors on the cancer cell membrane), and MRI. Therefore, the tumor (magnetic) targeting efficiency of magnetic iron oxide nanoparticles can be monitored by MRI; and these nanoparticles alone can inhibit tumor growth through several modals besides PTT. When combined as dual- or multimodal therapy, these magnetic iron oxide-based therapy methods can result significantly superior to a single therapy modal.

To further improve the tumor therapeutic efficiency, chemotherapy drugs, photosensitizer molecules, gold nanomaterials, semiconductor nanocrystals, other therapeutic drugs, and nanomaterials can be combined with magnetic iron oxide nanoparticles. The magnetic nanocomposites obtained can inhibit tumor growth through PTT, chemotherapy, photodynamic therapy, chemodynamic therapy, and other therapy modals. These multifunctional magnetic nanocomposites may also exhibit multimodal imaging such as MRI, fluorescent imaging, computed tomography, and photoacoustic imaging.

Although magnetic iron oxide nanoparticles-based PTT has numerous advantages, its shortcomings are also numerous. Magnetic iron oxide nanoparticles in aqueous solutions usually aggregate with each other. Also, after intravenous injection, these nanoparticles may cause cardiotoxicity in animals and patients. Further, after being treated with a higher dose of such nanoparticles, normal cells can also exhibit cytotoxicity. For tumor-targeted PTT, a higher dose of magnetic iron oxide nanoparticles should be injected into blood vessels since their photothermal conversion efficiency is lower than some other photothermal agents like  $\text{Cu}_{7.2}\text{S}_4$  and polypyrrole nanoparticles. Before clinical application, a deep investigation of the associated disadvantages should be carried for their redressal.

In this book, I focused on magnetic iron oxide nanoparticles-mediated cancer PTT through intratumoral or/and intravenous injection. The intratumoral injection benefits, the main factors affecting the retention of materials and permeability in solid tumors, have been discussed. Furthermore, an attempt has been carried to explore the performance of magnetic iron oxide nanoparticles after intravenous injection for tumor-targeted PTT based on several strategies [EPR effect, the conjugation of tumor-targeting ligands (active targeting), magnetic targeting under an external magnetic field, and multimodal targeting]. Also, the later part probes the gaps to improve the magnetic iron oxide nanoparticles-mediated PTT through intratumoral and intravenous injection modes. At the same time, it also includes the

current controversy on the EPR effect as well. In addition, discussion on drug-loaded magnetic nanocomposites, magnetic iron oxide/Au nanocomposites, and magnetic iron oxide/semiconductor nanocrystal nanocomposites for combination of cancer therapy and enhanced cancer PTT has also been included as an integral part.

The most investigated photothermal agents, including noble metal nanoparticles especially gold nanostars, carbon-based nanoparticles especially carbon nanotubes and graphitic carbon nanocages, black phosphorous nanosheets, conjugated polymer nanoparticles, and organic dye nanoparticles are also summarized. The requirements of an ideal photothermal agent and the advantages of magnetic iron oxide nanoparticles for cancer PTT have been discussed.

All contents were written by Maoquan Chu (储茂泉), a Professor working at Tongji University in China. This book may be suitable for undergraduate and post-graduate students, clinical doctors, basic research personnel, researchers and developers, and may also be ideal for technical non-specialists.

Shanghai, China  
Nov. 12, 2022

Maoquan Chu (储茂泉)

# Contents

<b>1</b>	<b>Photothermal Conversion Materials and Requirements for Ideal Photothermal Materials</b> . . . . .	1
1.1	Introduction . . . . .	1
1.2	Photothermal Materials . . . . .	3
1.2.1	Noble Metal Nanoparticle-Mediated Photothermal Therapy . . . . .	4
1.2.2	Carbon-Based Nanoparticles . . . . .	7
1.2.3	Metal-Containing Semiconductor Quantum Dots . . . . .	8
1.2.4	Black Phosphorous Nanosheets . . . . .	11
1.2.5	Others . . . . .	11
1.3	Requirements for Cancer Photothermal Materials . . . . .	13
1.4	Discussion . . . . .	14
	References . . . . .	16
<b>2</b>	<b>Advantages of Magnetic Iron Oxide Nanoparticles for Cancer Photothermal Therapy</b> . . . . .	23
2.1	Introduction . . . . .	23
2.2	Magnetic Iron Oxide Nanoparticles Have Been Used for Clinical Imaging, Drug-Targeted Delivery, and Cancer Therapy . . . . .	25
2.3	Magnetic Iron Oxide Nanoparticles Have a Broad Optical Absorption Band and Exhibit Highly Photothermal Stability . . . . .	27
2.4	Magnetic Iron Oxide Nanoparticles Deliverance to Target Tissue Through the Guidance of an External Magnetic Field . . . . .	29
2.5	Magnetic Iron Oxide Nanoparticles Are Delivered to Target Tissue Through the Guidance of both an External Magnetic Field and Active Targeting Biomolecules . . . . .	31
2.6	MRI Can Monitor the Tumor Targeting of the Magnetic Iron Oxide Nanoparticles . . . . .	33



2.7	Magnetic Iron Oxide Nanoparticle-Mediated PTT Can Be Combined with Magneto-Mechanical Force to Improve Cancer Therapy Efficiency. . . . .	34
2.8	Magnetic Iron Oxide Nanoparticle-Mediated PTT Can Be Combined with the Death Receptor-Induced Apoptosis to Improve Cancer Therapy Efficiency. . . . .	35
2.9	Combination of Laser-Triggered PTT and Alternating Magnetic Field-Induced Hyperthermia Can Improve the Iron Oxide Nanoparticle-Mediated Thermal Therapy Effect . . . . .	36
2.10	Discussion . . . . .	37
	References. . . . .	38
<b>3</b>	<b>Magnetic Iron Oxide Nanoparticles via Intratumoral Injection for Cancer Photothermal Therapy . . . . .</b>	<b>43</b>
3.1	Introduction . . . . .	43
3.2	The Advantages of Intratumoral Injection for Nanoparticle-Mediated Cancer Therapy . . . . .	44
3.3	Intratumoral Injection Is an Important Administration Route of a Drug in Clinical Practice . . . . .	45
3.4	The Main Factors on the Retention Effect of Materials in Tumor Tissue After Intratumoral Injection . . . . .	45
3.5	Magnetic Iron Oxide Nanoparticles via Intratumoral Injection for Cancer PTT . . . . .	50
3.6	Discussion . . . . .	53
	References. . . . .	54
<b>4</b>	<b>Magnetic Iron Oxide Nanoparticles via Intravenous Injection for Cancer Photothermal Therapy . . . . .</b>	<b>59</b>
4.1	Introduction . . . . .	59
4.2	The Enhanced Permeability and Retention Effect of Nanoparticles in Solid Tumor . . . . .	60
4.3	Magnetic Iron Oxide Nanoparticles Without Tumor-Targeting Ligands for Tumor-Targeted PTT . . . . .	62
4.3.1	Preventing the Immune System from Rapidly Cleaning Magnetic Iron Oxide Nanoparticles from the Circulation System. . . . .	68
4.3.2	Improving the Crystallinity of the Magnetic Iron Oxide Nanoparticles. . . . .	69
4.4	Magnetic Iron Oxide Nanoparticles Conjugated with Tumor-Targeting Ligands for Tumor-Targeted PTT . . . . .	70
4.5	Magnetic Iron Oxide Nanoparticles for Tumor-Targeted PTT Based on Magnetic Targeting . . . . .	72
4.6	Magnetic Iron Oxide Nanoparticles for Tumor-Targeted PTT Based on Both Active Targeting and Magnetic Targeting . . . . .	74
4.7	Discussion . . . . .	76
	References. . . . .	78

<b>5</b>	<b>Laser-Triggered Drug-Loaded Magnetic Iron Oxide Nanoparticles for Cancer Therapy</b> .....	85
5.1	Introduction .....	85
5.2	Drug-Loaded Magnetic Nanoparticles for Cancer Combined “PTT + Chemotherapy” .....	88
5.3	Drug-Loaded Magnetic Nanoparticles for Combined Cancer “PTT + PDT” or “PTT + PDT + Chemotherapy” .....	94
5.4	Discussion .....	97
	References .....	99
<b>6</b>	<b>Laser-Triggered Hybridize Magnetic Iron Oxide/Semiconductor Nanocrystals for Cancer Therapy</b> .....	105
6.1	Introduction .....	105
6.2	Fe <sub>3</sub> O <sub>4</sub> -“Heavy Metal-Based Semiconductor Nanocrystals” Hybridized Nanocomposites .....	110
6.2.1	Fe <sub>3</sub> O <sub>4</sub> -CuS Nanocomposites .....	110
6.2.2	Fe <sub>3</sub> O <sub>4</sub> -PbS/CdS Nanocomposites .....	112
6.2.3	Fe <sub>3</sub> O <sub>4</sub> -MoSe <sub>2</sub> Nanocomposites .....	113
6.3	Fe <sub>3</sub> O <sub>4</sub> -“Non-Heavy Metal-Based Semiconductor Nanocrystals” Hybridized Nanocomposites .....	117
6.4	Discussion .....	119
	References .....	120
<b>7</b>	<b>Hollow Mesoporous Copper Sulfide Nanoparticles for Cancer Phototherapy</b> .....	123
7.1	Introduction .....	123
7.2	Preparation of Hollow Mesoporous Copper Sulfide Nanoparticles .....	124
7.3	Optical Absorption Properties of Copper Sulfide Nanoparticles .....	127
7.4	Drug-Loaded Hollow Mesoporous Copper Sulfide for Cancer Therapy via the Combination of Photothermal Effect and Chemotherapy .....	129
7.5	Drug-Loaded Hollow Mesoporous Copper Sulfide for Cancer Therapy via the Combination of Photothermal/Chemodynamic Effect and Chemotherapy .....	133
7.6	Drug-Loaded Hollow Mesoporous Copper Sulfide for Cancer Therapy via the Combination of Photothermal/Photodynamic Effects, Chemodynamic Effect, and Chemotherapy .....	135
7.7	Discussion .....	137
	References .....	139
<b>8</b>	<b>Gold Nanostars for Cancer Photothermal Therapy</b> .....	143
8.1	Introduction .....	143
8.2	Gold Nanoparticles .....	144

8.3	Optical Properties of GNSs . . . . .	146
8.4	Photothermal Conversion of GNSs . . . . .	148
8.5	Photothermal Therapy . . . . .	152
8.6	Discussion . . . . .	155
	References. . . . .	156
<b>9</b>	<b>Laser-Triggered Hybridize Magnetic Iron Oxide/Gold Nanoparticles for Cancer Therapy . . . . .</b>	<b>161</b>
9.1	Introduction . . . . .	161
9.2	Magnetic Iron Oxide Nanoparticles Coated with an Au Nanoshell with a Smooth or Less Sharp Surface. . . . .	165
9.3	Magnetic Iron Oxide Nanoparticles Coated with an Au Nanoshell with Much Rough or Sharp Surface . . . . .	171
9.4	Discussion . . . . .	173
	References. . . . .	175
<b>10</b>	<b>Carbon Nanotubes for Cancer Photothermal Therapy. . . . .</b>	<b>177</b>
10.1	Introduction . . . . .	177
10.2	Photothermal Conversion of CNTs . . . . .	180
10.3	SWCNTs for Cancer Photothermal Therapy . . . . .	183
10.4	MWCNTs for Cancer Photothermal Therapy . . . . .	187
10.5	Discussion . . . . .	189
	References. . . . .	191
<b>11</b>	<b>Graphitic Carbon Nanocages for Cancer Photothermal Therapy . . . . .</b>	<b>193</b>
11.1	Introduction . . . . .	193
11.2	Preparation Methods of Carbon Nanocages . . . . .	195
11.3	Graphitic Carbon Nanocages for Cancer Photothermal Therapy . . . . .	199
11.3.1	808-nm Laser-Triggered CNCs for Cancer Photothermal Therapy . . . . .	199
11.3.2	980-nm Laser-Triggered CNCs for Cancer Photothermal Therapy . . . . .	202
11.4	Discussion . . . . .	204
	References. . . . .	204
<b>12</b>	<b>Black Phosphorous Nanosheets for Cancer Phototherapy . . . . .</b>	<b>207</b>
12.1	Introduction . . . . .	207
12.2	The Structure, Preparation Methods, and Biomedical Applications of BP Nanosheets . . . . .	208
12.3	Photothermal Conversion of BP Nanosheets and BPQDs. . . . .	211
12.4	BP Nanosheets and BPQDs for Cancer Photothermal Therapy . . . . .	216
12.5	Discussion . . . . .	221
	References. . . . .	224

<b>13 Organic Nanoparticles for Cancer Phototherapy</b> .....	229
13.1 Introduction .....	229
13.2 Polymer Nanoparticles for Cancer Photothermal Therapy .....	230
13.3 Nanoparticles Encapsulated with Organic Fluorescent Dyes for Cancer Photothermal Therapy.....	235
13.4 Discussion .....	240
References.....	241

## About the Author



**Maoquan Chu** (储茂泉) was born in Anhui Province in China. He received his PhD in Chemical Engineering from East China University of Science and Technology in 2001. He then did his postdoctoral work in the School of Life Science and Technology in Shanghai Jiaotong University, where he delved into biomaterials and nanotechnology. In 2004, he attended the School of Life Science and Technology at Tongji University. In 2007, he won the China Education Ministry's "New Century Excellent Talents Supporting Plan." In 2008, he was hired as a Professor and PhD supervisor. He is now a principal investigator at the School of Life Science and Technology, Frontier Science Center for Stem Cell Research, Tongji University and also at the Shanghai East Hospital in China. His main area of research is nanobiomedicine, with a current focus on cancer therapy using nanobiomaterials and cells. His recent research work has been published in many important journals such as *Small*, *Biomaterials*, *Acta Biomaterialia*, *Nano Research*, *Theranostics* and *ACS Applied Materials & Interfaces*. He has also published three books on biomaterials in early 2017.

# Chapter 1

## Photothermal Conversion Materials and Requirements for Ideal Photothermal Materials



**Abstract** Thermal therapy has been commonly selected for treating various tumors in a clinic for many years. Compared to traditional thermal therapy, photothermal conversion material-mediated photothermal therapy (PTT) induced by laser irradiation is a novel technique for the local treatment of tumors, which has several advantages over the traditional technique, such as selective heating on tumor tissue and fewer injuries in normal tissues. The PTT technique has shown rapid development in recent years, and many photothermal materials have been found or fabricated. These materials originate both naturally and synthetically, including organic and inorganic materials and organic/inorganic hybridized composites. For thermal therapy, the typically employed photothermal materials and the requirements of an ideal photothermal material have been discussed in this chapter. PTT-induced immunotherapy and photothermal materials combined with other therapeutic reagents for improving therapeutic efficiency have also been discussed.

**Keywords** Photothermal materials · Requirements for cancer photothermal materials · Photothermal therapy · Combination therapy · Limitations of photothermal therapy

### 1.1 Introduction

Once the structures of proteins, phospholipids, and other intracellular components are damaged, the structures and functions of cells and tissues/organs may be irreversibly changed. Thermal stimuli are an effective approach to damage cells, as the proteins and phospholipids in cells all exhibit low thermal stability. For example, when the cells are heated to at least  $\sim 40$  °C but no more than 45 °C, the intracellular enzyme is deactivated, which may induce irreversible cell injury. Cell death may occur if the cells are heated to about 42–43 °C [1]. When the temperature reaches 43–45 °C (or higher), and the duration of thermal stimuli reaches from 25 min to several hours, the cells may die because of the more serious injury of biomacromolecules as the deactivation of the enzyme [2]. For another example, the

leakage of intracellular  $K^+$  ions significantly increases with the temperature of heat treatment ranging from 46 to 54 °C [3]. Since it is widely known that cancer cells are continually increasing, the cells in the mitosis phase are more easily damaged by thermal stimuli. It can be attributed to why cancer cells are more susceptible to thermal stimuli than health cells [4]. Cancer cells may undergo apoptosis at temperatures ranging from 42 to 45 °C, while normal cells may live in this temperature range [5, 6].

Similarly, tumor tissues are more susceptible to thermal stimuli than normal tissues. It may be because the architectures of blood vessels and lymphatics in tumor tissue are abnormal compared to those in normal tissue (i.e., the lymphatic and blood reflux in tumors are reduced), resulting in easier heat accumulation within tumor tissue than in normal tissue. On the other hand, tumor blood flow in tumor tissue may be further reduced during heat treatment at high temperatures, reducing oxygen, nutrient supply, and acidosis [7]. Therefore, cancer cells can be killed, and heat treatment can inhibit tumor growth effectively.

Based on the temperature ranges, thermal therapy can be divided into two types: hyperthermia (~42–45 °C) and thermal ablation (>50 or 60 °C) [7–11]. Tumor tissue being either exposed to a lower temperature (>42 °C) for a long time or a higher temperature for a short time (e.g., a few minutes) shall encounter irreversible damage. For example, cancer cells will be killed after being treated with heat at 42–45 °C for 15–60 min or at >50 °C for only >4–6 min [12]. Based on the thermal exposure area, thermal therapy can be performed in three ways: whole body, regional, and local hyperthermia. Whole-body therapy is suitable for killing cancer cells in primary, metastatic tumors, and circulating cancer cells. Regional and local thermal therapies are suitable for rapidly killing cancer cells in a small localized tumor at the body's superficial position while avoiding damage to normal tissues. More than six types of energy sources, including thermal conduction-based devices, current, radiofrequency, microwave, ultrasound, and laser, have been introduced for generating heat in thermal cancer therapy. To improve the thermal effect in tumor tissue and reduce the thermal damage on normal tissue, thermal conversion materials, such as microwave thermal materials [13] and photothermal materials [14–17], have shown intensive development. The number of materials for significantly improving the efficiencies of microwave thermal therapy and thermal ultrasound therapy is limited. However, any blue, deep brown, gray, or black color can convert red or near-infrared (NIR) laser light into heat, reflecting the great potential for acting as photothermal materials.

Unlike to traditional laser-induced thermal therapy, organic dye molecule—and nanoparticle-mediated photothermal therapy (PTT) does not require a high-power laser source. This is because the tissue containing many photothermal materials upon laser irradiation will be damaged, as the temperature only in this tissue increases after exposure to the laser (i.e., selective heating) (Fig. 1.1). As mentioned above, all cancer cells would be damaged when the temperature reaches a critical value. Therefore, materials-mediated PTT may account for only a few thermal injuries to normal tissues, making it suitable for all solid tumor therapy with the properties of noninvasiveness and minimal or no drug resistance.

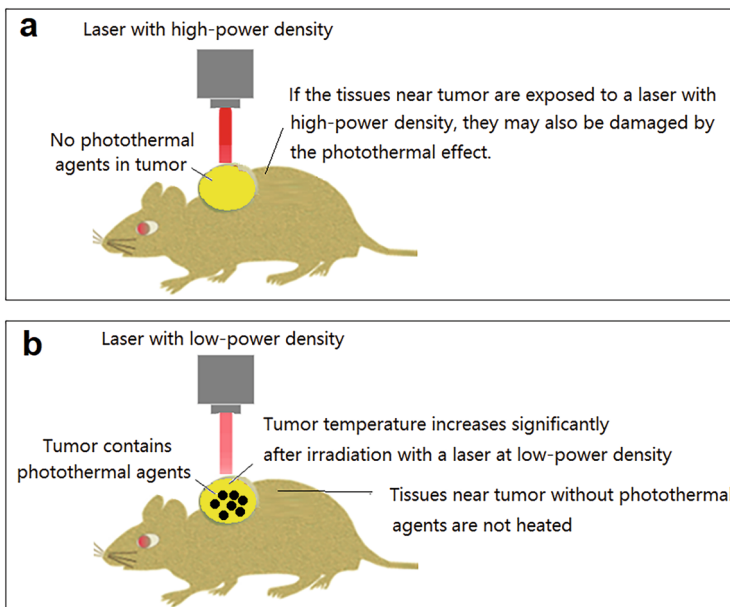


**Fig. 1.1** The difference between traditional laser-induced thermal therapy and material-mediated PTT. (a) Traditional laser-induced PTT (high-power laser should be used). (b) Photothermal material-mediated PTT (low-power laser satisfies the therapy). Photothermal material-mediated PTT has few injuries on normal tissue due to the low powder density of the applied laser

This technique has been investigated intensively in recent years, and many photothermal materials have been developed. The primary requirements for photothermal materials include good biocompatibility, high photothermal conversion efficiency, and good photostability (the additional requirements are described in Sect. 1.2). In this chapter, the main photothermal material types are summarized.

## 1.2 Photothermal Materials

Generally, any material with a high light absorption coefficient in red or NIR regions and low toxicity can be selected as photothermal materials for disease treatment, especially cancer therapy. To improve the homogeneity of heat distribution in tissue such as tumors and improve the tissue-targeted delivery of the photothermal materials, the size of photothermal materials should be in the nanometer-scale or small molecular range. In early 2003, gold nanoshells containing silica cores were developed and introduced into cancer PTT [18]. Over the following 18 years, numerous organic dyes and inorganic nanoparticles have been developed or are found to be used for PTT. These materials include noble metal nanoparticles, carbon-based nanoparticles, semiconductor quantum dots, magnetic iron oxide nanoparticles,



black phosphorous nanosheets, polymer nanoparticles, organic dyes, and so on (Fig. 1.2).

### 1.2.1 Noble Metal Nanoparticle-Mediated Photothermal Therapy

Noble metals comprise gold (Au) (serial number: 79, atomic mass: 197 g/mol), silver (Ag) (serial number: 47, atomic mass: 107.9 g/mol), and platinum-group metals. The latter further includes ruthenium (Ru) (serial number: 44, atomic mass: 101.1 g/mol), rhodium (Rh) (serial number: 45, atomic mass: 102.9 g/mol), palladium (Pd) (serial number: 46, atomic mass: 106.4 g/mol), osmium (Os) (serial number: 76, atomic mass: 190.2 g/mol), iridium (Ir) (serial number: 77, atomic mass: 192.2 g/mol), and platinum (Pt) (serial number: 78, atomic mass: 195.1 g/mol), as well as copper (Cu) (serial number: 29, atomic mass: 63.5 g/mol), rhenium (Re) (serial number: 75, atomic mass: 186.2 g/mol), and mercury (Hg) (serial number: 80, atomic mass: 200.6 g/mol). Most of them are in vivid color (e.g., yellow gold). When the sizes of these metals decrease to the nanoscale, their original color gets lost and appears gray or black.

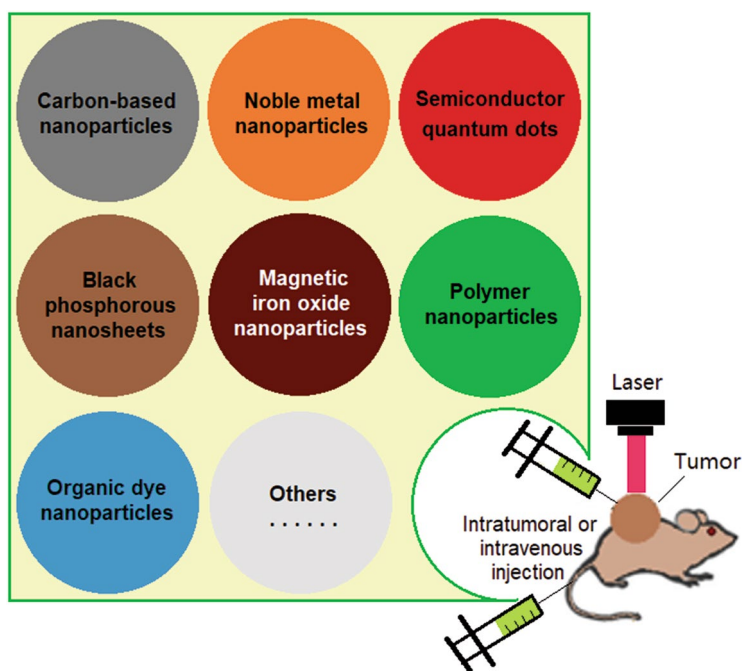
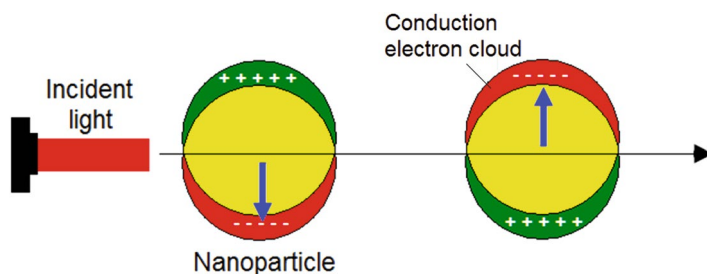


Fig. 1.2 Photothermal materials for cancer PTT through intratumoral or intravenous injection

Noble metals have a high concentration of free charge carriers ( $\sim 10^{23}/\text{cm}^3$  [19]). This is mainly why noble metal nanoparticles usually exhibit high photothermal conversion efficiency upon laser irradiation. The main mechanism of the photothermal conversion of the metal nanoparticles is due to the localized surface plasmon resonance (LSPR). When the gold nanoparticles or other metal nanoparticles are excited with a light, free electrons of the metal particles will be induced to collective coherent oscillation on the particle surface; as the electrons do not escape from the Coulomb force between the electrons and holes, these electron-hole pairs (i.e., dipoles) will simultaneously oscillate in a specific direction (the electric field of the incident light) [20, 21] (Fig. 1.3). When the frequency of these oscillated plasmas around the particle surface matches that of the incident light, the amplitude of the oscillated plasmas reaches a maximum value, and surface plasmon resonance (SPR) thus occurs. The smaller the nanoparticle size, the more plasma is on the particle surface. If the nanoparticle size is much smaller than the wavelength of the incident light, the plasma oscillation is confined in a very limited place; LSPR takes place under such conditions.

Nanoparticles in the different mediums have different LSPR frequencies (the lower the dielectric constant of the surrounding medium, the more significant the LSPR frequency). The LSPR frequency is also the function of metal nanoparticles' charge density, electronic charge, and effective mass [19]. The electronic charge density on the particle surface is determined by the metal particle's size, shape, type, and composition. Therefore, the LSPR properties of metal nanoparticles are dependent upon these properties. For example, on tailoring the shape of Au nanoparticles from spherical and rod to star-like shapes, the maxima LSPR peak significantly shifts from  $\sim 525$  nm through near 800 nm to near 850 nm (Fig. 1.5) [23].

LSPR has been used for various applications, such as surface analysis by plasmon-enhanced Raman spectroscopy [24], biomedical detection by biosensing [25], and photocatalysis [26]. As the incident light triggers the oscillated plasmas in metal nanoparticles, it releases a large amount of heat that makes LSPR widely useful for applications such as cancer therapy through photothermal conversion [27–33].



**Fig. 1.3** Surface plasma resonance of a nanoparticle induced by the oscillating electromagnetic field of an incident light

Gold (Au) nanostructures are first and commonly selected as photothermal agents for cancer PTT [34, 35]. Besides nano Au, nanoscale Ag [36], Au/Ag bimetallic composites [37], Pt [38], Au/Pt bimetallic composites [39], Cu [40], Cu/Au bimetallic composites [41], Pd [42], PdCu/Au composites [43], Re [44], etc., have been introduced into the PTT research field. Most reports focusing on these materials are basic studies that remain limited until the laboratory.

Biodegradable nanoparticles for cancer PTT are more lucrative than inert and non-biodegradable nanoparticles. In 2019, Zha and coworkers developed PEGylated Re nanoclusters for cancer PTT, which were degradable noble metal-based nanoparticles [44]. The as-synthesized Re nanoclusters were irregularly spherical with a hydrodynamic diameter of  $\sim 7.6$  nm (Fig. 1.4a).  $\text{H}_2\text{O}_2$  or  $\text{O}_2$  could oxidize these nanoclusters, and the oxidative products ( $\text{ReO}_4^-$ -ions) (Fig. 1.4b) could be cleaned from the body. Under 808-nm laser irradiation, the temperature of Re aqueous suspensions increased rapidly (Fig. 1.4c), and the photothermal conversion efficacy reached 33.0%. This strong photothermal effect could efficiently inhibit mouse tumor growth (Fig. 1.7d). Using low or no toxic and biodegradable nanoparticles as photothermal materials is a progressive trend in the cancer PTT field.

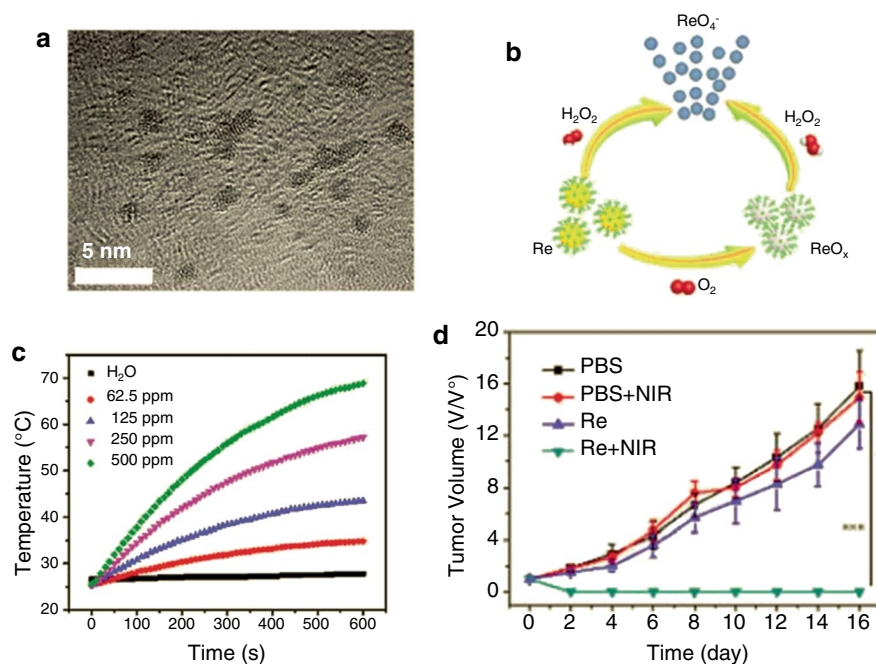


**Fig. 1.4** Degradable Re nanoclusters for cancer PTT. (a) TEM image. (b) Schematic illustration of degradation of Re in  $\text{H}_2\text{O}_2$  solution. (c) Photothermal conversion of different concentrated Re nanoclusters under 808-nm laser irradiation ( $2 \text{ W/cm}^2$ ) and control. (d) Tumor growth curves in different groups. A tumor (grew from 4 T1 cells)-bearing mice were intratumorally injected with Re nanoclusters ( $2 \text{ mg/mL}$ ,  $25 \text{ mL}$  for each tumor), followed by 10 min of an 808-nm laser ( $1 \text{ W/cm}^2$ ) irradiation. (Copyright © 2019 The Royal Society of Chemistry. Reprinted with permission from ref. [44])

### 1.2.2 Carbon-Based Nanoparticles

Carbon-based materials include 0-dimension carbon (e.g., fullerene, first reported in 1985), 1-dimension carbon (e.g., carbon nanotube, first reported in 1991), 2-dimension carbon (e.g., graphene, first reported in 2004), and 3-dimension carbon (e.g., carbon nanocages). These carbon-based materials have different bonds between carbon atoms. Therefore, carbon materials also can be divided into four types:  $sp^2$  hybrid structures (graphite, carbon nanotube, and graphene),  $sp^2$  and  $sp^3$  hybrid structures (amorphous carbon),  $sp^3$  hybrid structures (diamond), and  $sp$  hybrid structures (carbon chain) [46]. During the past decades, carbon-based materials have been intensively studied in many fields, such as energy conversion and storage, supercapacitor electrode materials, drug delivery, and cancer therapy due to their abundant microstructures and excellent physical-chemical properties, such as high stability and intrinsic conductivity. Carbon materials with brown, gray, or black colors can all act as photothermal materials for cancer PTT. Compared to noble metal nanoparticles, most of the carbon-based materials are low cost and low cytotoxic as well as exhibit easy processing and stable photothermal conversion. Therefore, these materials, such as photothermal, have attracted much attention in recent years. Up to now, graphene-based carbon materials (e.g., carbon nanotubes, reduced graphene oxide) [47, 48], activated carbon [22], and other carbon-based materials in black color [48] have been introduced into cancer PTT.

After carbonizing, organic macromolecules and plants such as natural wood, bamboo, and agricultural byproducts may change into brown, gray, or black products. Black activated carbon is a low-cost material that can be prepared using coconut shells, rice straw waste apricots, and other agricultural byproducts as precursors. These low-cost black materials can be used for cancer PTT. For example, when 200  $\mu\text{L}$  of nanoscale activated carbon made from bamboo (1 mg/mL) dispersed in polyvinylpyrrolidone (PVP) aqueous solution upon an 808 nm laser irradiation (power density, 0.25 W/cm<sup>2</sup>) increased from initial  $25.5 \pm 0.2$  °C to more than 39 °C after a 3 min irradiation, and to more than 53 °C after a 20 min irradiation; upon a 650 nm laser irradiation (power density, 0.5 W/cm<sup>2</sup>), the temperature of activated carbon aqueous suspension increased more rapidly than that of suspension upon an 808 nm laser irradiation [22]. For PVP-dispersed carbon nanotubes with the same concentration as above upon the same 650 nm and 808 nm laser irradiation, the temperatures after a 20 min irradiation were very close to those of activated carbon suspension [22].

Most carbon-based materials usually contain numerous porous lightweight, which are suitable for acting carriers for loading drugs and dual- or multi-modal therapy. For example, zinc phthalocyanine (ZnPc) could be incorporated into nanoscale activated carbon made from bamboo, and this drug-loaded activated carbon upon a 655 nm laser irradiation could kill cancer cells through the photothermal effect of activated carbon and the photodynamic effect of ZnPc (Fig. 1.5) [22].

It should be noted that most carbon-based materials are chemically inert, which makes them hard to be biodecomposed in vivo. Therefore, the intratumoral injection may be more suitable for carbon materials in vivo PTT than intravenous injection.

### 1.2.3 Metal-Containing Semiconductor Quantum Dots

Semiconductor QDs at an early stage (before ~2004) mainly refer to the metal-containing nanocrystals, including cadmium (Cd)-based QDs (e.g., CdSe) and Cd-free QDs (e.g., CuInS<sub>2</sub>). When the size of QDs is no more than the Bohr radius, a significant quantum size effect can be detected [49, 50]. These metal-containing QDs have unique optical properties, including high fluorescent QYs, high photostability, broad continuous excitation spectra, and narrow symmetric fluorescent emission spectra [49–51].

In recent years, novel QDs without metals, including graphene QDs, carbon QDs, polymer QDs, silicon QDs [52], and black phosphors QDs, have been intensively investigated due to their low toxicity compared to metal-containing QDs. This section discusses only the traditional QDs (i.e., metal-containing QDs) as photothermal materials.

Traditional semiconductor QDs are metalloid-crystal nanostructures with very small sizes ranging from ~1–10 nm. These nanocrystals are composed of elements from different groups such as group II(B)–VI(A) elements (e.g., CdTe), group III(A)–V(A) elements (e.g., InAs), group IV(A)–VI(A) elements (e.g., PbS), group

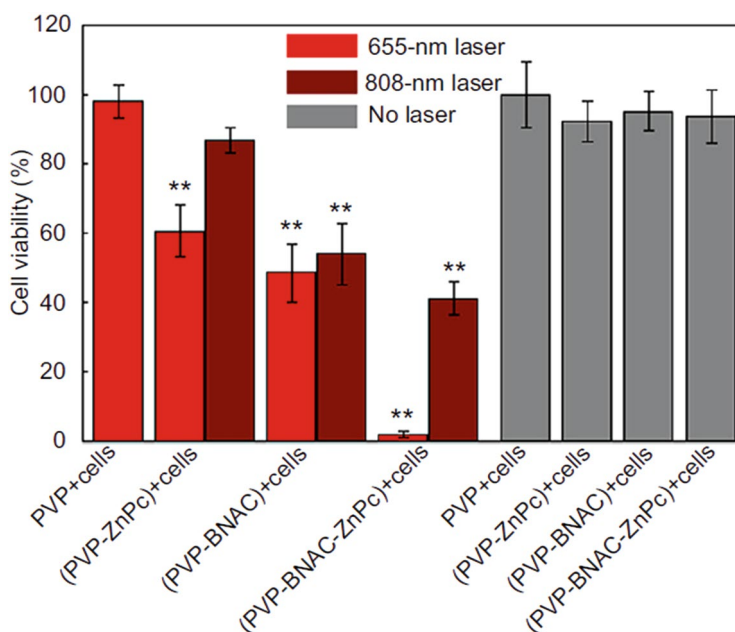


**Fig. 1.5** ZnPc-loaded activated carbon killing H-1299 cancer cells upon a 655 nm or 808 nm laser irradiation and controls. The samples were stabilized by PVP and dispersed in a cell culture medium. BNAC is bamboo nanoscale activated carbon. The concentrations of BNAC and ZnPc were 0.5 and 0.01 mg/mL, respectively. (Copyright © 2012 Elsevier Ltd. Reprinted with permission from ref. [22])

II(B)–VI(A) elements (e.g., ZnSe), group I(B)–VI(A) elements (e.g., AgS), or group I(B)–III(A)–VI(A) elements (e.g., CuInSe<sub>2</sub>).

The optical properties of QDs are size-dependent owing to their strong quantum size effect. The energy gap between the valence and conduction bands significantly increases with the reduced particle size (Fig. 1.6a). The larger the energy gap, the longer the absorption and fluorescent emission wavelengths. For example, the true-color fluorescence of CdTe QDs changed from green to red as the diameter of CdTe increased from small to large, ranging from ~1.5 to 3.5 nm, and the fluorescence and absorption peaks precisely shifted to a longer wavelength region with an increasing diameter (Fig. 1.6b) [53]. For another example, the absorption peaks of PbSe QDs significantly shifted to a longer wavelength in the NIR-II window (~1000–1700 nm) and close to the mid-infrared (MIR) region when the PbSe size increased from 3.3 to 8.1 nm (Fig. 1.6c) [54]. The optical properties of QDs are also dependent on the chemical composition. For example, the fluorescence wavelength regions of CdSe, CdTe, InP, and PbSe range from ~470 to 660 nm, from ~520 to 750 nm, from ~620 to 720 nm and more than 1000 nm, respectively (Fig. 1.6d) [55].

Compared to noble metal nanoparticles, QDs are not ideal plasmonic nanomaterials, as their electron charge densities are lower than those of metal nanoparticles. However, the charge densities of QDs can be changed [(10<sup>19</sup>–10<sup>21</sup>)/cm<sup>3</sup>] by chemical doping or specific post-reactions such as electrochemical reactions [56]. In addition, as mentioned above, the LSPR peak of QDs can shift to NIR or even MIR

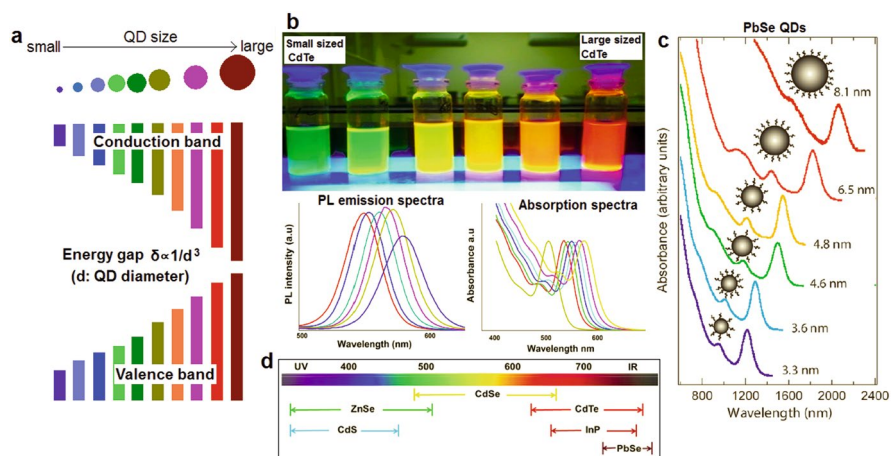


**Fig. 1.6** The optical properties of QDs are dependent on size and components. (a) Schematic illustration of quantum size effect. Upper: QD size increases from small to large, lower: energy gap between the valence and conduction bands is inversely proportional to the cube of QD diameter. (b) Fluorescence, emission, and absorption spectra of CdTe QDs. (Copyright © 2017 Elsevier B.V. Reprinted with permission from ref. [53].) (c) Absorption spectra of PbSe QDs and the corresponding particle size (schematic illustration). (Copyright © 2012 Elsevier Ltd. Reprinted with permission from ref. [54].) (d) Fluorescence emission wavelength regions of different QDs (schematic illustration). (Copyright © 2019 Elsevier B.V. Reprinted with permission from ref. [55])

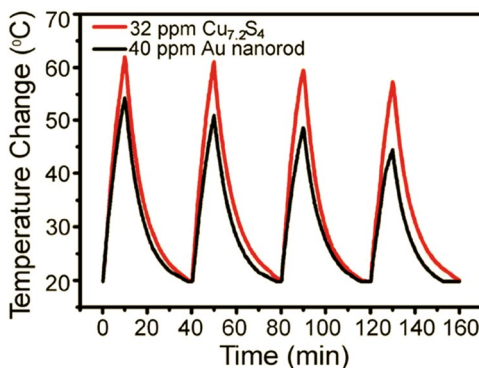
regions. Therefore, QDs have been widely used as photothermal materials for cancer PTT.

In early 2010, Li et al. reported that spherical CuS nanocrystals could convert 808 nm laser light into heat energy [57]. Since then, the photothermal conversion of numerous semiconductor QDs for cancer PTT has been investigated. These QDs include CdTe [58], hydrophilic flower-like CuS [59], Cu<sub>9</sub>S<sub>5</sub> [60, 61], Cu<sub>7.2</sub>S<sub>4</sub> [45], Cu<sub>2</sub>(OH)PO<sub>4</sub> [62], Ag<sub>2</sub>S [63–65], Ag–Ag<sub>2</sub>S–CdS hybrid nanocrystals [66], Ag<sub>2</sub>Se [67], MoS<sub>2</sub> [68], WS<sub>2</sub> [69, 70], V<sub>2</sub>C [71], antimonene [72], etc. The photothermal conversion efficiency of semiconductor QDs can reach over 50% [45, 59]. For example, the photothermal conversion efficiency of the cubic structured Cu<sub>7.2</sub>S<sub>4</sub> nanocrystals (~20 nm) irradiated with a 980-nm laser was measured to be 56.7%, which was significantly higher than that of gold nanorods (under the 980-nm laser: 24.6%, under the 808-nm laser: 35.8%) [45]. In addition, the photothermal stability of the Cu<sub>7.2</sub>S<sub>4</sub> nanocrystals was more promising than that of the gold nanorods (Fig. 1.7) [45]. However, the photothermal conversion stability also decreased with prolonged laser irradiation times.

QDs under laser irradiation at a suitable wavelength other than emitting fluorescence and converting the incident light energy into heat also generate toxic ROS. In early 2003, Samia et al. reported that CdSe QDs in toluene solution under 488-nm excitation could produce singlet oxygen (<sup>1</sup>O<sub>2</sub>) with ~5% quantum yield [73]. Although the quantum yield of <sup>1</sup>O<sub>2</sub> is much lower than the classic photosensitizer (e.g., the quantum yield of <sup>1</sup>O<sub>2</sub> generated by Pc4 photosensitizer reached 43% [74]), the exhibited optical properties of semiconductor QDs are more stable than those of classic photosensitizers.

Other types of metal-containing QDs, especially transition metal dichalcogenide (TMD) nanosheets, such as MoS<sub>2</sub>, have also been intensively investigated for cancer PTT. A detailed description of the related content is in Chap. 6.

**Fig. 1.7** Comparison of the photothermal stability of Cu<sub>7.2</sub>S<sub>4</sub> nanocrystals and gold nanorods over four on/off cycles of 980-nm laser irradiation (2 W). (Copyright © 2014 The Royal Society of Chemistry. Reprinted with permission from ref. [45])



### 1.2.4 *Black Phosphorous Nanosheets*

Although heavy metal-containing semiconductor QDs can be used simultaneously as PTT and PDT materials, these nanocrystals are only suitable for loading drugs if these QDs are fabricated into hollow/porous structures. Due to their high cytotoxicity, these semiconductor QDs may have few opportunities to be applied in the human body. Gold nanostructures such as gold nanocages and carbon-based nanoparticles such as graphene oxide can be used for loading drugs and possess relatively lower cytotoxicity than the semiconductor QDs. Still, most of these nanomaterials can be used only as PTT materials, as little or only low-level ROS can be generated after laser irradiation (except GQDs). Compared with the gold nanostructure, carbon-based nanoparticles, and semiconductor QDs, black phosphorous (BP) not only exhibits low cytotoxicity but can also be used simultaneously as PTT and PDT materials, drug carriers as well as immune-potentiating nanoadjuvant [75–82].

BP is a two-dimensional (2D) semiconductor with a unique structure and a new type of phototherapy agent. Like the QDs mentioned in Sect. 3.3, BP quantum dots (BPQDs) (ultra-small BP nanosheets with the size of several nanometers) can also emit bright fluorescence (usually green color); for example, the fluorescence quantum yield reaches 10.2% when BPQDs were excited by a 355 nm light [83]. Therefore, besides their functions, including drug delivery and cancer therapy, BPQDs can also be used for fluorescent imaging.

It should be noted that BP is not stable in air, in water, and upon light exposure. Bare BP is not suitable for acting as a photothermal agent or other biomedical application. BP surface should be covered with a shell through physical encapsulation or chemical reaction before application [84–87]. Nano BP has high biocompatibility and biodegradability. As phosphorous is a necessary trace element, BP's degradation products are not harmful to the body, making BP potentially suitable for clinical trials, such as phototherapy.

### 1.2.5 *Others*

Polymeric materials have been intensively investigated in the nanomedicine research field. Polymer acting as a photothermal material is interesting research, as some polymers are good biocompatible and biodegradable *in vivo* when compared to inorganic photothermal materials. Electron-type conductive or semiconducting polymers are usually used as polymer photothermal agents [88–95]. These polymer-based PTT agents include polyaniline, polypyrrole, polythiophene, etc. The advantages of these polymer agents are low cytotoxicity and biodegradability, as well as good photostability.

Organic dyes with high red or NIR absorption coefficients have attracted much attention, as most of them can be used simultaneously as photothermal and



photodynamic agents for cancer PDT/PTT. Some organic dyes can be used for *in vivo* imaging, such as fluorescent imaging and photoacoustic imaging.

These organic dyes are small molecules. For example, the molecular weight of indocyanine green (ICG), the most commonly used NIR cyanine dye and commonly used PTT agent [96], is 774.97. These molecular dyes can be easily cleaned from the body after administration due to their small size (this rapid body clearance is beneficial for reducing the toxicity accumulation in the body; however, it also decreases the accumulation of dyes in target tissue such as tumors due to the rapid blood clearance).

Natural organic dyes can also be used as photothermal agents for cancer PTT [97–99]. The sources of the natural PTT agents are abundant and low toxicity. For example, melanin can be extracted in large quantities from black sesame shells (Fig. 1.8 [98]), and chlorophyll can be extracted from all green vegetables. Both black sesame and green vegetables can be easily obtained from the marketplace. Upon an 808 nm laser irradiation (0.8 W), the temperature of HCl-hydrolyzed melanin (extracted from *mytilus edulis* shells) in water increased rapidly, and the photothermal conversion efficiency reached 22.89% (Fig. 1.9) [97]. Except for melanin, most organic dyes are not stable in color after laser irradiation. For example, methylene blue is a common blue dye that has been used in clinical practice for more than 120 years [100]. Upon laser irradiation, methylene blue with higher concentration can simultaneously generate ROS and heat [101]. However, the photothermal effect decreases after long-term laser irradiation as methylene blue is decomposed after irradiation.

**Fig. 1.8** Melanin powder extracted from black sesame shells. (Copyright © 2016 Elsevier Ltd. Reprinted with permission from ref. [98])

